

# Machine Learning-Driven Analysis of Suspension Parameter Effects on Two-Wheeler and rider Vibrations on Class C Roads

J.B.Ashtekar<sup>1</sup>, Ajaykumar Thakur<sup>1</sup>, M.P.Nagarkar<sup>2</sup>

<sup>1</sup>ashtekarjaydeep@yahoo.in, ajay\_raja34@yahoo.com, Sanjivani College of Engineering, Kopargaon,

<sup>2</sup>Smt Kashibai Navale College of Engineering, Pune

## ARTICLE INFO

Received: 20 Dec 2024

Revised: 02 Feb 2025

Accepted: 18 Feb 2025

## ABSTRACT

The dynamic behavior of a two-wheeler suspension system significantly affects ride comfort, stability, and human body vibrations, especially on uneven road surfaces. This study offers a mathematical modeling and simulation analysis of a two-wheeler with a seated rider navigating a Class C road profile, in accordance with ISO 8608 requirements. The model integrates essential suspension characteristics, such as tire stiffness (both front and rear), suspension spring stiffness (both front and rear), and damping coefficients (both front and rear), which were methodically altered to examine their effects on vehicle and rider dynamics. A Simulink-based multi-degree-of-freedom (MDOF) system was created to mimic vertical acceleration and displacement reactions across many body parts, including the head, upper torso, lower torso, viscera, and seat. A parameter sweep was performed across 729 distinct suspension configurations, and the resulting time-domain responses were analyzed to determine the maximum acceleration and displacement magnitudes for each body location.

Multiple regression-based modeling techniques were utilized to numerically describe the impact of suspension parameters on the observed biomechanical responses. The efficacy of many regression models was assessed to determine a precise predictive correlation among suspension stiffness, damping characteristics, and the resulting rider acceleration and displacement. The established models offer a computational framework for analyzing two-wheeler ride dynamics and serve as a basis for future research in suspension tuning, optimization, and human-centric ride comfort assessment.

**Keywords:** Vehicle-Rider Interaction, Suspension Stiffness and Damping, Vertical Acceleration Response, Biomechanical Vibration Analysis, Regression-Based Modelling, Simulink Suspension Simulation, Human Body Vibrations, ISO 8608

## 1.INTRODUCTION

Motorcycles are a favored means of transportation, especially over short distances, owing to their efficiency and capacity to maneuver through traffic. One major concern for motorcycle riders is exposure to whole-body vibration (WBV), which can lead to discomfort, musculoskeletal illnesses, and chronic health difficulties such as low back pain (LBP), neck pain, and spinal abnormalities. WBV is mostly induced by inconsistencies in road surfaces, which are conveyed to the rider via the motorcycle's suspension system. The transfer of vibrations can lead to considerable discomfort and may result in long-term health consequences for riders. Prior research has shown that whole-body vibration (WBV) exposure in motorcycles is significantly greater than in other vehicle categories, such as automobiles, mainly because of the direct interaction between the rider and the vehicle (Kumar et al., 2013; Saran et al., 2013; Eluri et al., 2019). As vehicle speed escalates or when navigating uneven road surfaces, the severity of whole-body vibration (WBV) intensifies, resulting in enhanced discomfort and an elevated risk of health issues, especially for professional riders subjected to these conditions for prolonged durations (Tathe et al., 2013; Chen et al., 2003).

The motorcycle's suspension system is essential for minimizing the transfer of vibrations from the road to the rider's body. Passive suspension systems, which do not actively adapt to road conditions, are frequently employed in

motorcycles; however, they usually inadequately deliver maximum comfort when the vehicle's load varies, such as with fluctuations in the rider's weight or road conditions. Researchers have discovered that these systems frequently fail to adequately mitigate vibrations, resulting in enhanced discomfort and health hazards for the rider (Nagarkar et al., 2016; Mitra et al., 2016). The suspension system must absorb road shocks to reduce vibrations transmitted through the bike frame and seat, hence improving comfort. Improvements in suspension design, including the integration of variable stiffness and damping properties, have demonstrated a substantial reduction in vibration transmission, hence enhancing comfort and safety (Nagarkar et al., 2016).

Besides suspension system attributes, rider posture and seat design are vital elements that affect WBV exposure and related discomfort. Studies have shown that inadequate seating arrangements and postures, such as slouching or suboptimal seating angles, may worsen the detrimental effects of whole-body vibration (WBV), especially on the lumbar spine (Amiri et al., 2019; Kumbhar et al., 2012). These postural tensions intensify discomfort, elevate the risk of spinal injury, and lead to tiredness. Conversely, an ergonomic seat design with enough support may reduce these consequences by equally dispersing the body's weight and diminishing pressure on critical areas. Specifically, seat angle, lumbar support, and the configuration of the seat cushion can substantially influence the level of whole-body vibration (WBV) exposure encountered by the rider (Tathe et al., 2013; Kumar et al., 2013).

Various biodynamic models have been created to examine the effects of WBV on riders. These models replicate the interaction between the human body and the motorcycle's suspension system, assisting researchers in forecasting the rider's reaction to varying vibration levels. The predominant models employed for these assessments consist of lumped-parameter models, finite element models, and multibody dynamics models. These models provide a comprehensive examination of vibration transmission from the suspension system to the rider's body and permit the modification of suspension parameters to mitigate WBV exposure (Mitra et al., 2016; Nagarkar et al., 2016). These models facilitate the assessment of suspension performance for vibration dose value (VDV), frequency-weighted RMS acceleration, and acceleration magnitudes at pivotal body areas, including the head and lumbar spine (Nagarkar et al., 2016; Kumar et al., 2013).

The impact of WBV on the rider can be assessed using objective metrics such as VDV and RMS acceleration, which are essential indications of rider comfort. Prior studies have formulated recommendations, including ISO 2631-1, to evaluate WBV exposure and its related health hazards. These standards specify safe exposure thresholds for different vehicle categories and circumstances. By integrating these criteria with biodynamic models, researchers can enhance suspension systems to decrease the rider's exposure to hazardous vibrations. This technique entails assessing the biomechanical responses of the rider and identifying the suspension characteristics (such as dampening and spring stiffness) that alleviate discomfort while preserving vehicle stability (Chen et al., 2003; Saran et al., 2013).

This study aims to examine the impact of whole-body vibration (WBV) exposure on rider comfort and health, specifically analyzing the correlation among suspension system characteristics, road conditions, and rider posture. The project aims to develop suspension systems to mitigate WBV exposure by merging advanced simulation tools with biodynamic models. This project investigates the application of machine learning techniques to forecast the impact of various suspension configurations on rider comfort, contributing in the creation of motorcycles that prioritize both comfort and health. The results of this study may guide future design enhancements, rendering motorbikes safer and more pleasant for riders, especially those in occupations necessitating prolonged riding exposure (Mansfield and Griffin, 2002; Mitra et al., 2016; Saran et al., 2013).

## 2.METHODOLOGY

A multi-degree-of-freedom (MDOF) model of a two-wheeler with a seated rider was developed in Simulink to replicate the system's dynamic behavior. The model incorporates the vehicle's suspension system, rider dynamics, and their interaction, utilizing the Class C road profile, as defined by ISO 8608 standards, as the input excitation for the suspension system to simulate road roughness. The suspension system was modeled utilizing many critical parameters: tire stiffness (kf), spring stiffness (kr), damping coefficients (cf, cr), and tire stiffness (kft, krt). The parameters were adjusted within designated ranges to produce a total of 729 distinct suspension configurations. Each configuration was simulated to capture the maximum vertical acceleration and displacement responses at several rider body regions, including the head, upper torso, lower torso, viscera, and seat. The simulation data were gathered for all 729 possibilities, recording the greatest acceleration and displacement at each body location. The data were structured into arrays, with each entry containing values for acceleration and

displacement related to the different suspension settings. (Fig 1) Regression models were built to analyse the relationship between suspension parameters and the rider's response. Feature selection was performed, utilizing the suspension settings as input features and the maximum acceleration and displacement as output responses. A variety of regression approaches were utilized, including Linear Regression, Support Vector Regression (SVR), Random Forest Regression, K-Nearest Neighbors (KNN) Regression, Decision Tree Regression, and Gradient Boosting Regression. The evaluation of model performance included standard metrics, including Mean Squared Error (MSE), R-Squared ( $R^2$ ), Root Mean Squared Error (RMSE), and Adjusted R-Squared. The regression model with the lowest error metrics and highest  $R^2$  was chosen for further study. After selecting the optimal regression model, it was evaluated by cross-validation procedures to confirm its robustness and generalizability. The resulting model was utilized to forecast the acceleration and displacement responses for any specified set of suspension settings. The regression model findings were meticulously examined to ascertain the impact of each suspension parameter on vertical acceleration and displacement at several rider body regions, specifically the head, upper torso, and lower torso. The influence of suspension stiffness, damping coefficients, and tire stiffness on rider comfort and safety was assessed. In conclusion, an optimization approach was implemented, suggesting the optimal suspension arrangement that reduces vertical acceleration and displacement at key body areas, hence improving ride comfort and mitigating health hazards linked to vibration exposure.

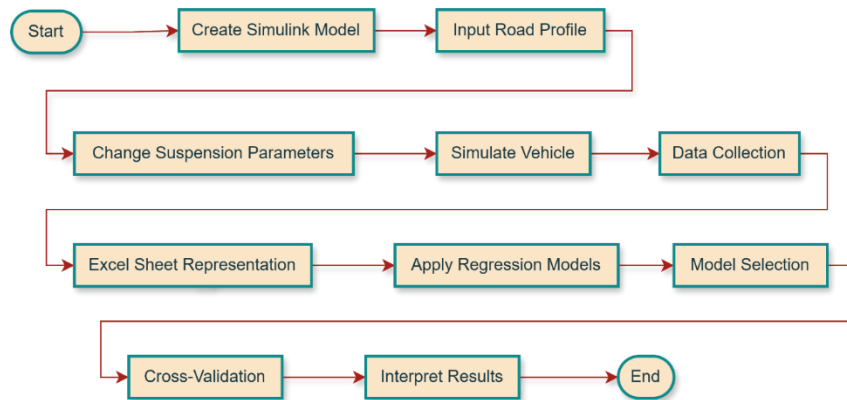


**Fig 1 Methodology**

### 3 SIMULINK MODEL

The developed Simulink model is a four degree-of-freedom dynamic system designed to simulate the biomechanical response of a seated human subject under vibratory excitation. The model represents the human body and its interaction with the seat through four interconnected dynamic elements. Each degree of freedom corresponds to a key segment: the head, upper torso, lower torso (or waist), and the seat. In addition to these, the model captures additional motion characteristics in the viscera and provides displacement outputs for the head, torso, and seat. (Fig 2)

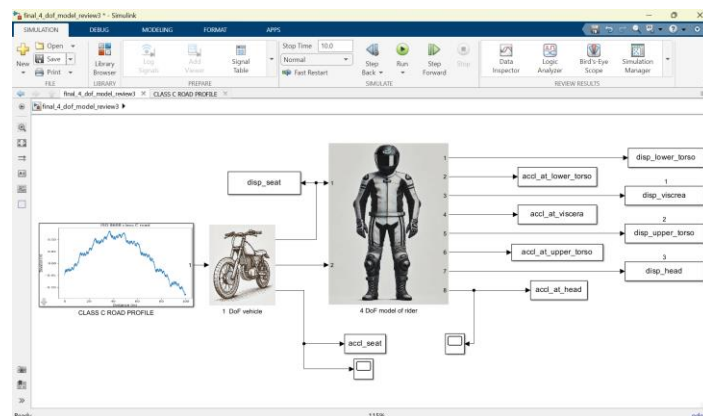


**Fig.2 Simulink Model**

### 3.1. Class C modelling based on ISO 8608

The International Standard ISO 8608 categorizes road roughness by the Power Spectral Density (PSD) of road elevation. Class C roads have moderate roughness, inferior to Class A/B but superior to Class D. The Power Spectral Density (PSD) function characterizes the roughness of a road surface. ISO 8608 models the road profile as a stochastic process using the following equation:

$$G_q(n) = G_{q0} \left( \frac{n}{n_0} \right)^{-\omega}$$

where

$$G_q(n) = \text{Power Spectral Density (PSD) of the road profile } \frac{m^3}{\text{cycle}} \frac{1}{m}$$

$$G_{q0} = \text{Reference PSD value at reference frequency } n_0 \left( 0.1 \frac{\text{cycles}}{m} \right)$$

$$n = \text{spatial frequency (cycles per meter)}$$

$$n_0 = \text{reference spatial frequency } \left( 0.1 \frac{\text{cycles}}{m} \right)$$

$$\omega = \text{Exponent (2)}$$

PSD Values for Class C road Classes (ISO 8608)

$$G_q(n) = (64 \times 10^{-6}) \left( \frac{n}{0.1} \right)^{-2}$$

A Band-Limited White Noise block produces a stochastic signal that emulates fluctuations in road roughness. The Noise Power is established at  $5 \times 10^{-6}$  Class C roughness intensity.

Since a raw random signal is unrealistic, we apply a transfer function filter to shape the spectrum (fig 5). The filter follows the ISO 8608 model:

$$H(s) = \frac{1}{s^2 + 2\zeta\omega_c s + \omega_c^2}$$

where:

$\omega_c = 2\pi \times 0.5$  rad/s (cutoff frequency),  $\zeta = 0.1$  (damping factor)

This eliminates artificial high-frequency elements and simulates actual road irregularities. The filtered signal is directed to an Output (Road Output), which may be linked to a car model's suspension system. Figure 3 illustrates the road profile for a 100-meter road sample.

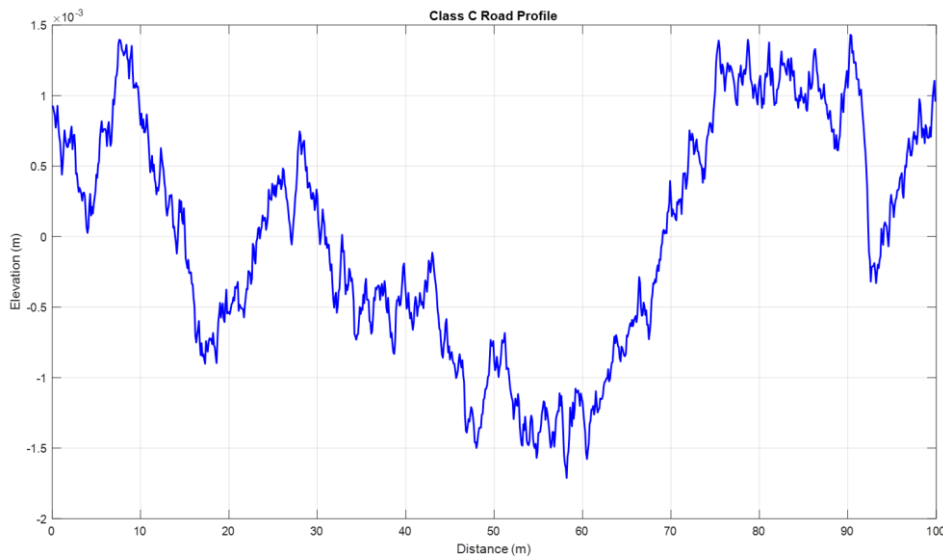


Fig3 .Road Profile for 100m road sample

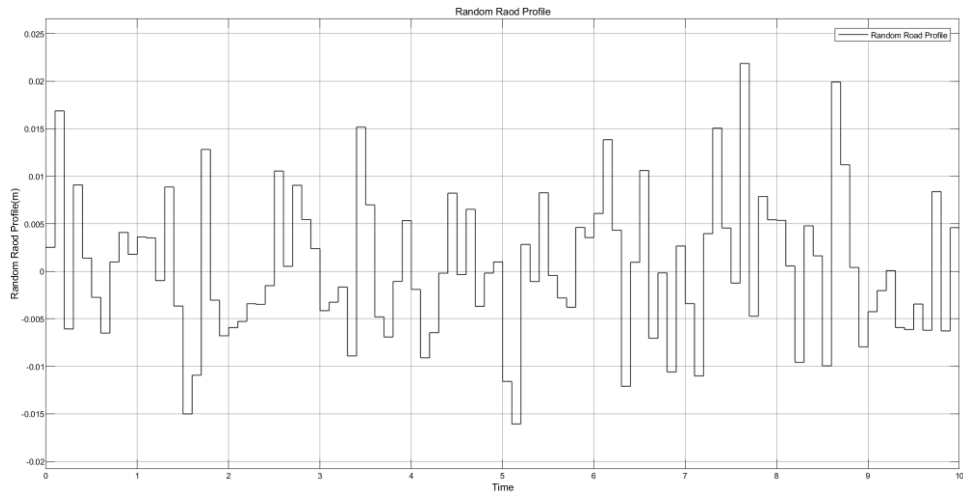


Fig 4. Random Road Profile

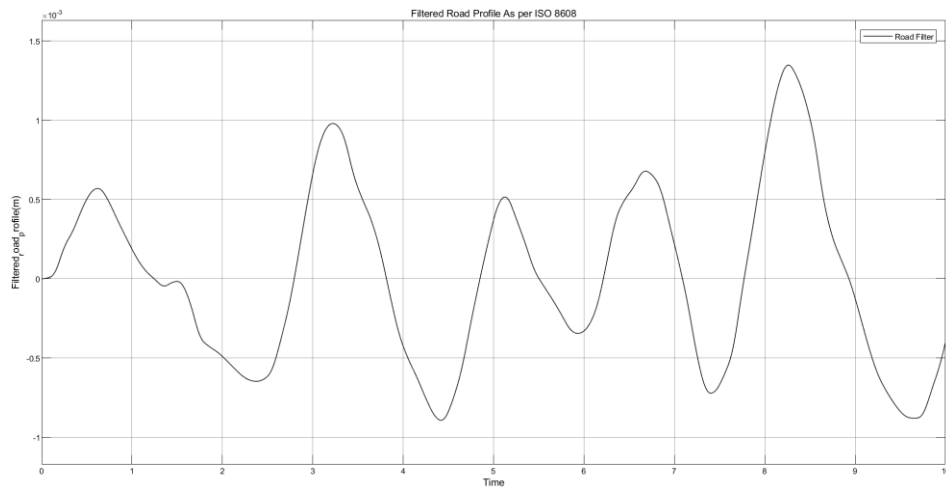


Fig 5. Filtered Road Profile

### 3.2 Two-wheeler single DoF model

For finding biodynamic responses of the model mass and geometric parameters of the model are required. In this study these parameters are taken from available literature. Single-degree-of-freedom model of the motorcycle as indicated in Fig. 6. (Rohidas Tathe, S., Wani, K. P., 2013)

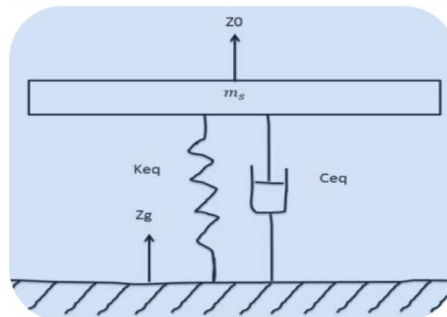


Fig 6 Two-wheeler single DoF model

The values of equivalent mass, equivalent stiffness and equivalent damping are calculated using following formulae

$$m_{eq} = m_s + m_r$$

$$c_{eq} = c_r + c_f$$

$$K_{eq} = \frac{k_f k_t}{k_f + k_{ft}} + \frac{k_r k_{rt}}{k_r + k_{rt}}$$

where,

For our simulation

$m_r = 70$  kg;

$m_s = 158.6$  kg;

$$m_{eq} \ddot{z}_0 + c_{eq}(\dot{z}_0 - \dot{z}_g) + k_{eq}(z_0 - z_g) = 0$$

Where,

$z_g$  = ground excitation displacement

### 3.3 Model of rider

#### Biodynamic model equation

Considering Wan & Schimmel's 4 DOF Model as shown in figure 7 following equations are developed. (Kumbhar, P. B., Xu, P., Yang, J., 2012)

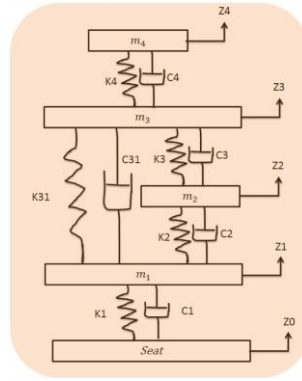


Fig 7 Four DOF Wan and Schimmels Model

For finding biodynamic responses of the model mass and geometric parameters of the model are required. In this study these parameters are taken from available literature as shown in table 1.

**Table 1. Model Parameters for Wan & Schimmels 4 DOF Model**

Mass(kg)	Damping(N-s/m)	Stiffness(N/m)
$m_1 = 36$	$c_1 = 2475$	$k_1 = 49340$
$m_2 = 5.5$	$c_2 = 330$	$k_2 = 20000$
$m_3 = 15$	$c_3 = 200$	$k_3 = 10000$
$m_4 = 17$	$c_4 = 250$	$k_4 = 134400$
	$c_{31} = 909.1$	$k_{31} = 192000$

$m_1$  = mass of lower torso

$m_2$  = mass of viscera

$m_3$  = mass of upper torso

$m_4$  = mass of head and neck

$c_1$  = damping coefficient between lower torso and seat

$c_2$  = damping coefficient between viscera and lower torso

$c_3$ = damping coefficient between viscera and upper torso

$c_4$ = damping coefficient between neck and upper torso

$c_{31}$ = damping coefficient between lower and upper torso

$k_1$ = stiffness between lower torso and seat

$k_2$ = stiffness between viscera and lower torso

$k_3$ = stiffness between viscera and upper torso

$k_4$ = stiffness between neck and upper torso

$k_{31}$ = stiffness between neck and upper torso

$$m_1 \ddot{z}_1 + c_1(\dot{z}_1 - \dot{z}_0) + c_{31}(\dot{z}_1 - \dot{z}_3) + c_2(\dot{z}_1 - \dot{z}_2) + k_1(z_1 - z_0) + k_{31}(z_1 - z_3) + k_2(z_1 - z_2) = 0 \dots \dots \dots (1)$$

$$m_2 \ddot{z}_2 + c_2(\dot{z}_2 - \dot{z}_1) + c_3(\dot{z}_2 - \dot{z}_3) + k_2(z_2 - z_1) + k_3(z_2 - z_3) = 0 \dots \dots \dots (2)$$

$$m_3 \ddot{z}_3 + c_{31}(\dot{z}_3 - \dot{z}_1) + c_3(\dot{z}_3 - \dot{z}_2) + c_4(\dot{z}_3 - \dot{z}_4) + k_{31}(z_3 - z_1) + k_3(z_3 - z_2) + k_4(z_3 - z_4) = 0 \dots \dots \dots (3)$$

$$m_4 \ddot{z}_4 + c_4(\dot{z}_4 - \dot{z}_3) + k_4(z_4 - z_3) = 0 \dots \dots \dots (4)$$

where

$z_0$ =seat displacement

$z_1$ =lower torso displacement

$z_2$ =viscera displacement

$z_3$ = upper torso displacement

$z_4$ =head and neck displacement

### 3.4 Responses of Simulink model

Following responses are collected from Simulink model. Suspension parameters are provided for it.(Fig 8)

For getting multiple inputs we used doepy. doepy is a library in python used to obtain full factorial design array of Design of Experiment (Sarkar, T. (2019)).As shown in table 2

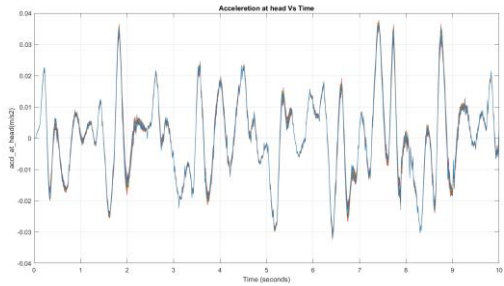
$k_f$ :[15000,16000,17000], $c_f$ :[640,740,840], $k_r$ :[70000,75000,80000]

$c_r$ :[2040,2140,2240], $k_{ft}$ :[150000,165000,180000] ,  $k_{rt}$ :[150000,165000,180000]

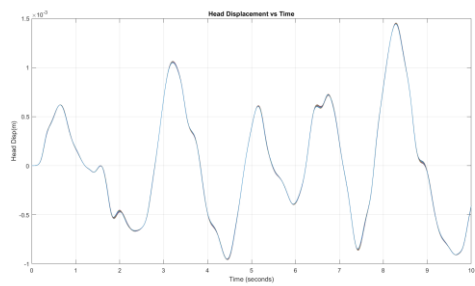
**Table 2. DoE table**

Sr.No.	$k_f$	$c_f$	$k_r$	$c_r$	$k_{ft}$	$k_{rt}$
1	15000	640	70000	2040	150000	150000
2	16000	640	70000	2040	150000	150000
3	17000	640	70000	2040	150000	150000
4	15000	740	70000	2040	150000	150000
5	16000	740	70000	2040	150000	150000
...	...	...	...	...	...	...
...	...	...	...	...	...	...
...	...	...	...	...	...	...
727	15000	840	90000	2240	180000	180000
728	16000	840	90000	2240	180000	180000

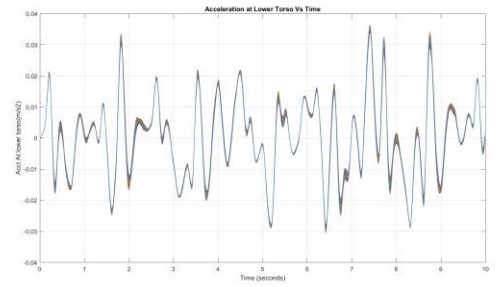
729	17000	840	90000	2240	180000	180000
-----	-------	-----	-------	------	--------	--------



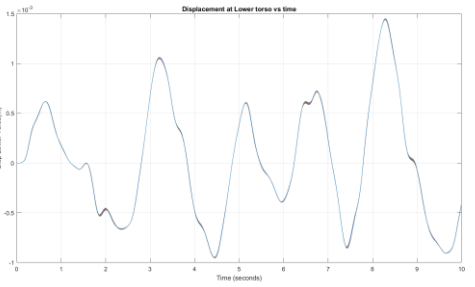
a) Acceleration at Head



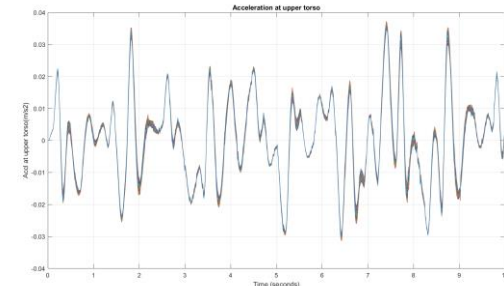
b) Displacement at Head



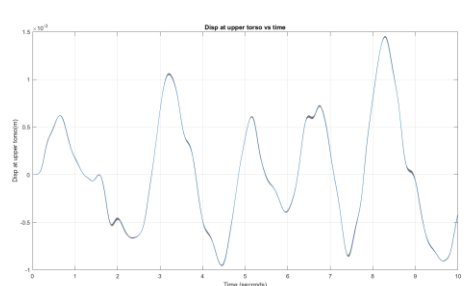
c) Acceleration at Lower Torso



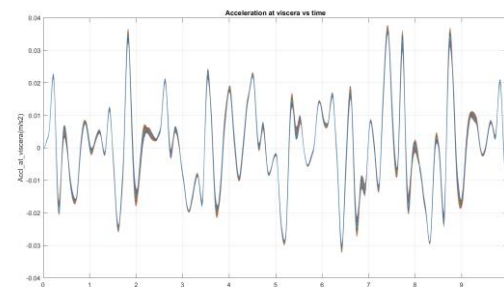
d) Displacement at Lower Torso



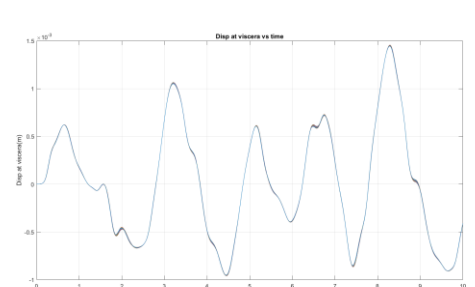
e) Acceleration at Upper Torso



f) Displacement at Upper Torso



g) Acceleration at Viscera



h) Displacement at Viscera





727	15000	840	90000	2240	180000	180000	0.0014	0.0014	0.0014	0.0014
728	16000	840	90000	2240	180000	180000	0.0014	0.0014	0.0014	0.0014
729	17000	840	90000	2240	180000	180000	0.0014	0.0014	0.0014	0.0014

## 4.2 Regression model explanation

Following regression model is used:

1. Linear Regression
2. Random Forest
3. Gradient Boosting
4. Support Vector Regression (SVR)
5. XG Boost

**Linear Regression** is a simple and interpretable method, assuming a linear relationship between the dependent and independent variables, and is suitable for predicting continuous outcomes. **Random Forest** is an ensemble method that builds multiple decision trees and averages their predictions, offering robustness against overfitting and the ability to handle complex, non-linear relationships. **Gradient Boosting** constructs trees sequentially, where each tree corrects errors from the previous ones, providing high accuracy for complex tasks but requiring careful tuning to prevent overfitting. **Support Vector Regression (SVR)**, based on the principles of Support Vector Machines, is effective for non-linear relationships and noise-resistant, though it can be computationally expensive. Lastly, **XGBoost** is a highly optimized variant of Gradient Boosting, known for its computational efficiency and regularization techniques, making it particularly effective for large-scale, high-performance regression tasks. Each of these models is chosen based on data complexity, accuracy requirements, and computational resources.

## 4.3 Model performance parameter

Following self-explanatory table shows performance measurements of all models.

**Table 4 Model Performance Parameters**

Metric	Description	Formula	Interpretation
R-squared ( $R^2$ )	Represents the proportion of variance explained by the model, ranging from 0 to 1.	$R^2 = 1 - \frac{\text{Sum of squared residuals}}{\text{Total sum of squares}}$	Higher values (closer to 1) indicate a better fit. However, it can be misleading when many predictors are added.
Adjusted R-squared (Adjusted $R^2$ )	Adjusted version of $R^2$ that accounts for the number of predictors in the model, penalizing unnecessary predictors.	$R^2 = 1 - \frac{(1 - R^2)(n - 1)}{(n - p - 1)}$ $n$ is the number of data points; $p$ is the number of predictors	A more reliable measure when comparing models with different numbers of predictors. Can be negative if the model is worse than a horizontal line.
Root Mean Squared Error (RMSE)	Measures the average magnitude of prediction errors, computed as the square root of the average squared differences between observed and predicted values.	$RMSE = \sqrt{\frac{1}{n} \sum_{i=1}^n (y_i - \hat{y}_i)^2}$ $y_i$ is the actual value. $\hat{y}_i$ is the predicted value.	Lower values indicate better accuracy. Sensitive to outliers as errors are squared.

## 4.4 Model Training and Performance Evaluation for Multiple Output Variables

In this study, various regression models were employed to predict multiple output variables, utilizing a set of input features. The input data, loaded from the "simulation\_results.xlsx" file, contains six predictor variables: **kf**, **cf**, **kr**, **cr**, **kft**, and **krt**. These variables represent different factors related to the system being studied. The target output variables are related to different types of accelerations and displacements in the human body, such as **max\_accl\_at\_head**, **max\_accl\_at\_lower\_torso**, **max\_accl\_at\_upper\_torso**, **max\_accl\_at viscera**, **max\_accl\_at\_seat**, **max\_head\_disp**, **max\_lower\_torso\_disp**, **max\_seat\_disp**, and **max\_upper\_torso\_disp**. Each output corresponds to the measurement of acceleration or displacement at various body parts under certain conditions.

To evaluate the effectiveness of the models in predicting these output variables, the data was split into training and testing sets, with 80% of the data used for training the models and 20% reserved for testing the models' predictive capabilities. This partitioning of the dataset helps ensure that the models are tested on unseen data, providing a more accurate assessment of their generalization ability.

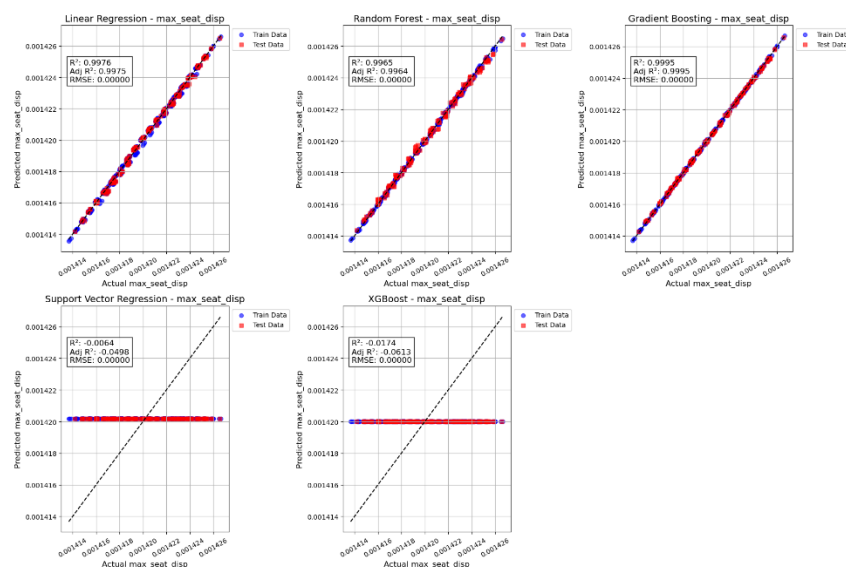
The models tested in this study include **Linear Regression**, **Random Forest**, **Gradient Boosting**, **Support Vector Regression (SVR)**, and **XGBoost**, which are popular regression algorithms used in machine learning tasks. Each model was trained on the training set using the six input features to predict the target output variables. These models were selected due to their ability to handle both linear and non-linear relationships between the input and output variables. After training the models, predictions were made on both the training and testing datasets to assess their performance.

For each output variable, scatter plots were generated to visually compare the actual versus predicted values for both the training and testing data. The scatter plots display the relationship between the observed (actual) values and the predicted values, with different markers representing training and testing data points. These plots help illustrate how well the models generalize from the training data to the unseen test data. A reference line ( $y = x$ ) was included in the plots to provide a baseline for perfect predictions. The closer the points are to this line, the better the model's predictions are.

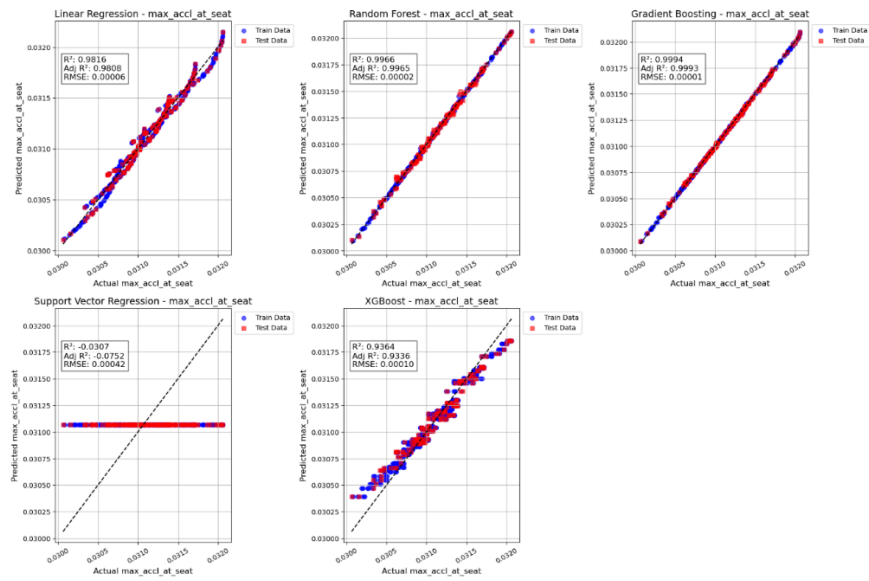
In addition to the scatter plots, key performance metrics were computed for each model and output variable to quantitatively evaluate the models' effectiveness. These metrics include **R-squared ( $R^2$ )**, which measures the proportion of the variance in the target variable that is explained by the model; **Adjusted R-squared**, which adjusts the  $R^2$  value based on the number of predictors in the model, penalizing unnecessary predictors and making it a better measure for comparing models with different complexities; and **Root Mean Squared Error (RMSE)**, which provides an estimate of the average magnitude of the errors made by the model in its predictions, with smaller values indicating better predictive accuracy.

The performance metrics were displayed in each plot, allowing for a direct comparison between the models. These metrics were calculated for both the training and testing sets, providing a comprehensive view of how well each model fits the data and how it performs on unseen data. The study also calculated **Adjusted  $R^2$**  for each model to account for the complexity of the model (i.e., the number of predictors used) and prevent overfitting, especially in models that include many features or when comparing models with varying numbers of predictors.

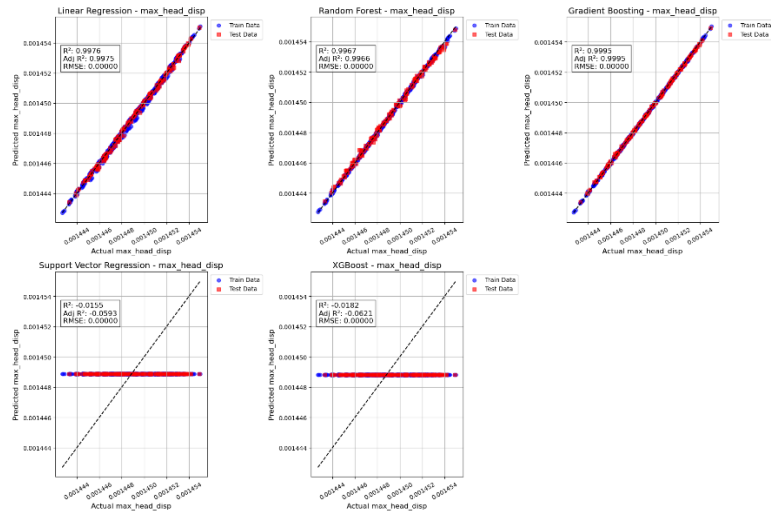
By evaluating the models on multiple output variables, this study provides a detailed assessment of the ability of each regression algorithm to predict physical measurements related to human body dynamics. The visual and quantitative analyses combined in this approach allow for a comprehensive evaluation of the model performance, which is crucial for selecting the most appropriate model for real-world prediction tasks, where both accuracy and interpretability are important. Following graphs a) to i) shows the actual vs predicted data and corresponding  $R^2$ , adjusted  $R^2$  and RMSE values.



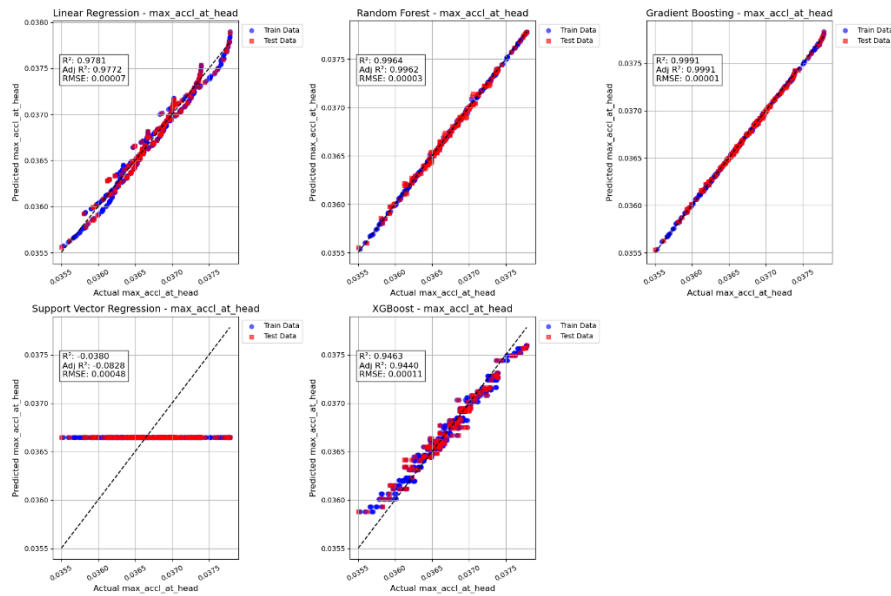
a) Displacement of seat



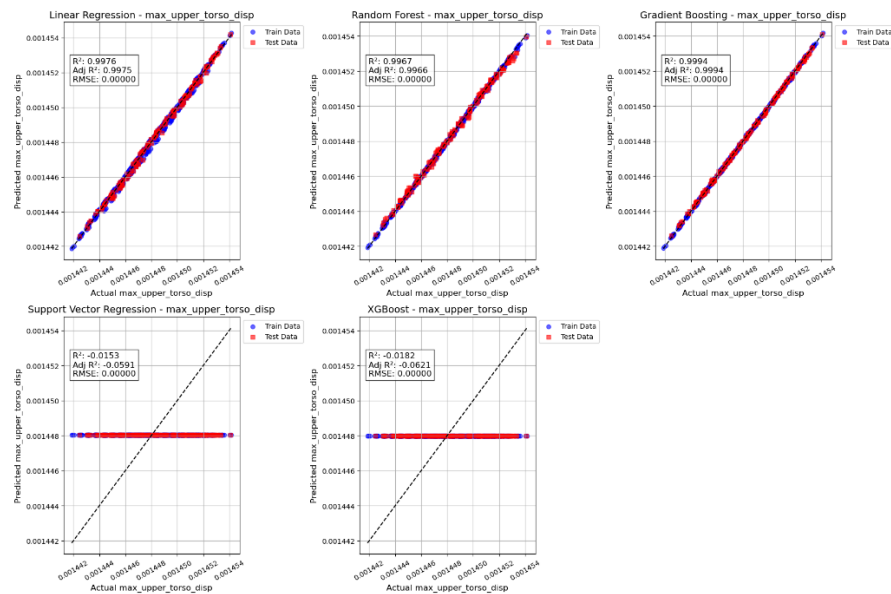
b) Acceleration of seat



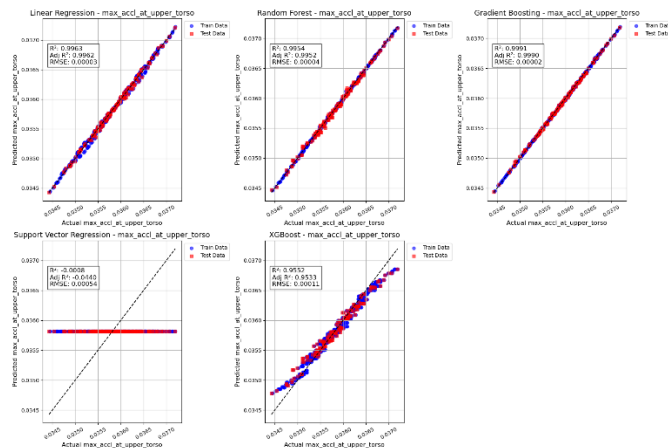
c) Displacement of Head



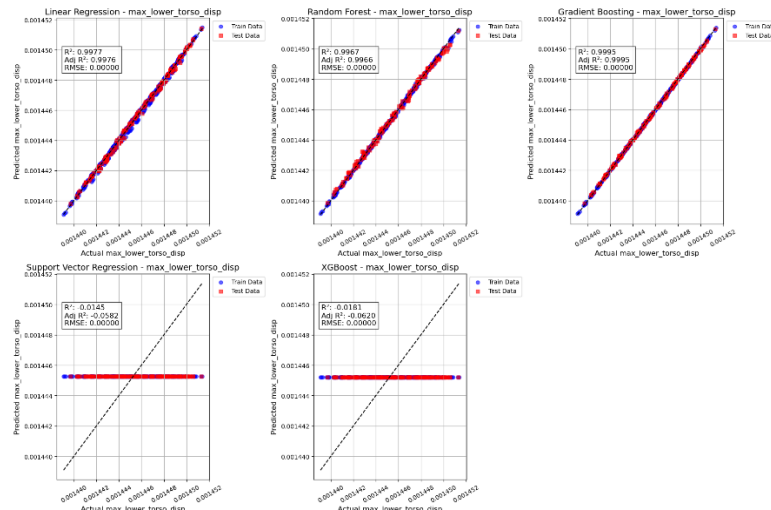
d) Acceleration of Head



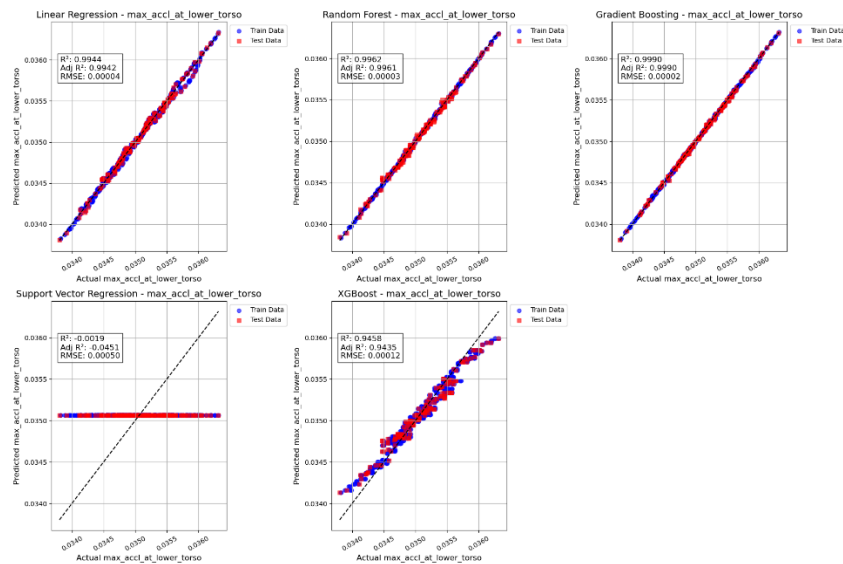
e) Displacement of Upper torso



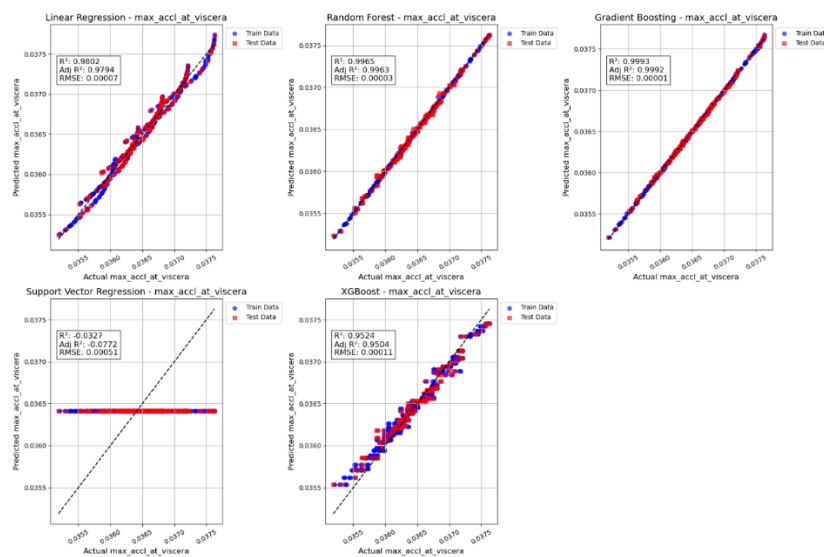
f) Acceleration of upper torso



g) Displacement of lower torso



h) Acceleration of Lower torso



i) Acceleration of Viscera

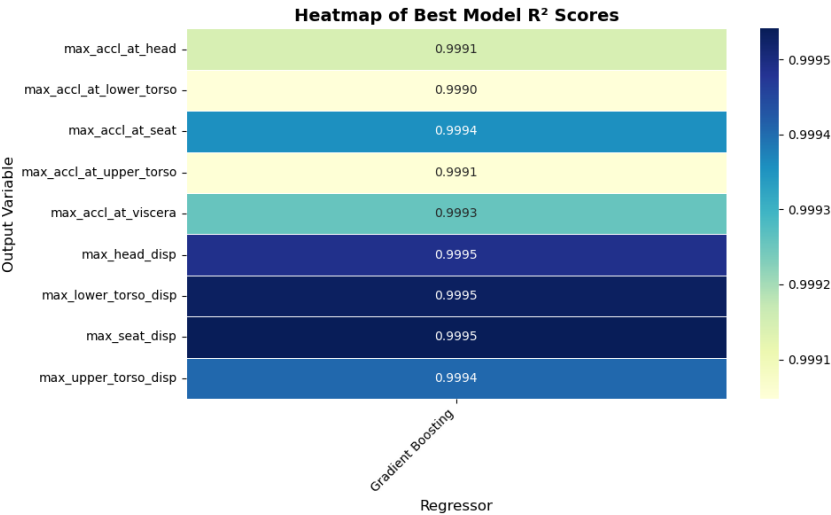
Regressor Performance:

Following self-explanatory table shows the performance of the regressor

Output Variable	Regressor	R <sup>2</sup> Score	Adjusted R <sup>2</sup>	RMSE
max_accl_at_head	Linear Regression	0.97813	0.97719	0.00007
max_accl_at_head	Random Forest	0.99638	0.99622	0.00003
max_accl_at_head	Gradient Boosting	0.99914	0.99911	0.00001
max_accl_at_head	Support Vector Regression	-0.03798	-0.08278	0.00048
max_accl_at_head	XGBoost	0.94628	0.94396	0.00011
max_accl_at_lower_torso	Linear Regression	0.99444	0.99420	0.00004
max_accl_at_lower_torso	Random Forest	0.99622	0.99606	0.00003
max_accl_at_lower_torso	Gradient Boosting	0.99905	0.99901	0.00002
max_accl_at_lower_torso	Support Vector Regression	-0.00185	-0.04510	0.00050
max_accl_at_lower_torso	XGBoost	0.94579	0.94345	0.00012
max_accl_at_upper_torso	Linear Regression	0.99633	0.99617	0.00003
max_accl_at_upper_torso	Random Forest	0.99541	0.99521	0.00004
max_accl_at_upper_torso	Gradient Boosting	0.99905	0.99901	0.00002
max_accl_at_upper_torso	Support Vector Regression	-0.00080	-0.04400	0.00054
max_accl_at_upper_torso	XGBoost	0.95523	0.95330	0.00011
max_accl_at viscera	Linear Regression	0.98022	0.97937	0.00007
max_accl_at viscera	Random Forest	0.99649	0.99634	0.00003
max_accl_at viscera	Gradient Boosting	0.99926	0.99922	0.00001
max_accl_at viscera	Support Vector Regression	-0.03267	-0.07725	0.00051
max_accl_at viscera	XGBoost	0.95244	0.95038	0.00011
max_accl_at_seat	Linear Regression	0.98158	0.98079	0.00006
max_accl_at_seat	Random Forest	0.99663	0.99648	0.00002
max_accl_at_seat	Gradient Boosting	0.99936	0.99933	0.00001
max_accl_at_seat	Support Vector Regression	-0.03072	-0.07521	0.00042
max_accl_at_seat	XGBoost	0.93635	0.93360	0.00010
max_head_disp	Linear Regression	0.99764	0.99754	0.00000
max_head_disp	Random Forest	0.99671	0.99657	0.00000
max_head_disp	Gradient Boosting	0.99949	0.99947	0.00000
max_head_disp	Support Vector Regression	-0.01549	-0.05932	0.00000
max_head_disp	XGBoost	-0.01817	-0.06212	0.00000
max_lower_torso_disp	Linear Regression	0.99768	0.99758	0.00000
max_lower_torso_disp	Random Forest	0.99675	0.99660	0.00000
max_lower_torso_disp	Gradient Boosting	0.99953	0.99951	0.00000
max_lower_torso_disp	Support Vector Regression	-0.01445	-0.05824	0.00000
max_lower_torso_disp	XGBoost	-0.01810	-0.06205	0.00000
max_seat_disp	Linear Regression	0.99760	0.99750	0.00000
max_seat_disp	Random Forest	0.99654	0.99639	0.00000
max_seat_disp	Gradient Boosting	0.99954	0.99952	0.00000
max_seat_disp	Support Vector Regression	-0.00636	-0.04980	0.00000

max_seat_disp	XGBoost	-0.01742	-0.06134	0.00000
max_upper_torso_disp	Linear Regression	0.99765	0.99755	0.00000
max_upper_torso_disp	Random Forest	0.99670	0.99656	0.00000
max_upper_torso_disp	Gradient Boosting	0.99941	0.99938	0.00000
max_upper_torso_disp	Support Vector Regression	-0.01526	-0.05909	0.00000
max_upper_torso_disp	XGBoost	-0.01816	-0.06210	0.00000

Best Model



Output Variable	Regressor	R <sup>2</sup> Score	Adjusted R <sup>2</sup>	RMSE
max_accl_at_head	Gradient Boosting	0.99914	0.99911	0.00001
max_accl_at_lower_torso	Gradient Boosting	0.99905	0.99901	0.00002
max_accl_at_seat	Gradient Boosting	0.99936	0.99933	0.00001
max_accl_at_upper_torso	Gradient Boosting	0.99905	0.99901	0.00002
max_accl_at viscera	Gradient Boosting	0.99926	0.99922	0.00001
max_head_disp	Gradient Boosting	0.99949	0.99947	0.00000
max_lower_torso_disp	Gradient Boosting	0.99953	0.99951	0.00000
max_seat_disp	Gradient Boosting	0.99954	0.99952	0.00000
max_upper_torso_disp	Gradient Boosting	0.99941	0.99938	0.00000

CONCLUSION

The regression analysis conducted on the simulation outputs demonstrates that ensemble methods, particularly Gradient Boosting and Random Forest, deliver exceptionally high predictive performance. With R<sup>2</sup> scores consistently approaching 0.999 and extremely low RMSE values, these models capture the underlying relationships in the data with near-perfect accuracy. Linear Regression also shows solid performance, albeit slightly lower than the ensemble methods, indicating its adequacy for simpler predictive tasks.

In contrast, Support Vector Regression (SVR) and XGBoost, as configured in this study, exhibit negative R<sup>2</sup> and Adjusted R<sup>2</sup> values for several output variables, which suggests that these models fail to outperform a naïve mean-based predictor without further hyperparameter tuning or methodological adjustments. Overall, the findings suggest that ensemble methods are the most robust choice for modelling the experimental outcomes in this context, while



simpler linear models provide a viable, interpretable alternative. The suboptimal performance of SVR and XGBoost indicates a need for further optimization if these approaches are to be considered for future predictive applications.

## REFERENCES

- [1] **Chen, H.-C., Chen, W.-C., Liu, Y.-P., Chen, C.-Y., Pan, Y.-T., 2009.** Whole-body vibration exposure experienced by motorcycle riders – An evaluation according to ISO 2631-1 and ISO 2631-5 standards. *Int. J. Ind. Ergon.* 39, 708–718. <https://doi.org/10.1016/j.ergon.2009.05.002>
- [2] **Rohidas Tathe, S., Wani, K. P., 2013.** SAE two-wheeler simulation. SAE Technical Paper 2013-01-2859
- [3] **Kumbhar, P. B., Xu, P., Yang, J., 2012.** A Literature Survey of Biodynamic Models for Whole Body Vibration and Vehicle Ride Comfort. *ASME Proc. IDETC/CIE*
- [4] **Singh, I., Nigam, S. P., Saran, V. H., 2014.** Modal analysis of human body vibration model for Indian subjects under sitting posture. *Ergonomics* 58(7), 1117–1132. <https://doi.org/10.1080/00140139.2014.961567>
- [5] **Kumar, V., Saran, V. H., Guruguntla, V., 2013.** Study of Vibration Dose Value and Discomfort due to Whole Body Vibration Exposure for a Two-Wheeler Driver. *Proc. 1st International and 16th National Conf. on Machines and Mechanisms (iNaCoMM 2013), IIT Roorkee, India*
- [6] **K. Wanjale, A. A. Deshmukh, J. C. Vanikar, A. P. Adsul and S. P. Bendale,** "Detecting Human Eye Blinks through OpenCV," *2024 IEEE 9th International Conference for Convergence in Technology (I2CT)*, Pune, India, 2024, pp. 1-5, doi: 10.1109/I2CT61223.2024.10543678,
- [7] **Mathivanan Durai, R. B. Dravidapriyaa, S.P. Prakash, Wanjale, K. H., M. Kamarunisha, & M. Karthiga. (2025).** Student Interest Performance Prediction Based On Improved Decision Support Vector Regression Using Machine Learning. *International Journal of Computational and Experimental Science and Engineering*, 11(1). <https://doi.org/10.22399/ijcesen.999>
- [8] **Parvez, M., Khan, A. A., 2019.** Prediction of Ride Comfort of Two-Wheeler Riders Exposed to Whole-Body Vibration. *Advances in Engineering Design*, Springer Nature Singapore Pte Ltd. [https://doi.org/10.1007/978-981-13-6469-3\\_52](https://doi.org/10.1007/978-981-13-6469-3_52)
- [9] **Arslan, Y. Z., 2014.** Experimental Assessment of Lumped-Parameter Human Body Models Exposed to Whole Body Vibration. *J. Mech. Med. Biol.* 15(1), 1550023. <https://doi.org/10.1142/S0219519415500232>
- [10] **Stenlund, T., Lundström, R., Lindroos, O., Rehn, B., Öhberg, F., 2020.** Seated postural loads caused by shock-type whole-body vibration when driving over obstacles. *Int. J. For. Eng.* <https://doi.org/10.1080/14942119.2020.1761745>
- [11] **Griffin, M. J., 1998.** A comparison of standardized methods for predicting the hazards of whole-body vibration and repeated shocks. *J. Sound Vib.* 215(4), 883–914. [https://doi.org/10.1016/S0022-460X\(98\)98160-0](https://doi.org/10.1016/S0022-460X(98)98160-0)
- [12] **Jugulkar, L. M., Singh, S., Sawant, S. M., 2016.** Analysis of suspension with variable stiffness and variable damping force for automotive applications. *Advances in Mechanical Engineering* 8(5), 1–19. <https://doi.org/10.1177/1687814016648638>
- [13] **Mitra, A. C., Soni, T., Kiranchand, G. R., 2016.** Optimization of automotive suspension system by design of experiments: A nonderivative method. *Adv. Acoust. Vib.* 2016, 3259026. <https://doi.org/10.1155/2016/3259026>
- [14] **Nagarkar, M. P., Vikhe Patil, G. J., Zaware Patil, R. N., 2016.** Optimization of nonlinear quarter car suspension–seat–driver model. *J. Adv. Res.* 7, 991–1007. <https://doi.org/10.1016/j.jare.2016.04.003>
- [15] **Nagarkar, M. P., El-Gohary, M. A., Bhalerao, Y. J., Vikhe Patil, G. J., Zaware Patil, R. N., 2019.** Artificial neural network prediction and validation of optimum suspension parameters of a passive suspension system. *SN Appl. Sci.* 1:569. <https://doi.org/10.1007/s42452-019-0550-0>
- [16] **Chicco, D., Warrens, M. J., Jurman, G., 2021.** The coefficient of determination R-squared is more informative than SMAPE, MAE, MAPE, MSE and RMSE in regression analysis evaluation. *PeerJ Comput. Sci.* 7:e623. <https://doi.org/10.7717/peerj-cs.623>
- [17] **Amiri, S., Naserkhaki, S., Parnianpour, M., 2019.** Effect of whole-body vibration and sitting configurations on lumbar spinal loads of vehicle occupants. *Comput. Biol. Med.* <https://doi.org/10.1016/j.compbiomed.2019.02.019>

- [18] **Kumar, V., Saran, V. H., Guruguntla, V., 2013.** Study of vibration dose value and discomfort due to whole body vibration exposure for a two-wheeler driver. *Proc. 1st International and 16th National Conf. on Machines and Mechanisms (iNaCoMM 2013), IIT Roorkee, India*
- [19] **Sarkar, T. (2019).** *doepy: Design of Experiment Generator in Python* (Version 0.0.1) <https://doepy.readthedocs.io/en/latest/>
- [20] International Organization for Standardization (ISO). (2016). *ISO 8608:2016 - Mechanical vibration — Road surface profiles — Reporting of measured data*. ISO. <https://www.iso.org/standard/71202.html>